Published in final edited form as:
J Bone Miner Metab. 2007 ; 25(6): 383–391. doi:10.1007/s00774-007-0774-8.

Frequency-dependent enhancement of bone formation in murine tibiae and femora with knee loading

Ping Zhang[1,2], **Shigeo M. Tanaka**[3], **Qiwei Sun**[1,4], **Charles H. Turner**[1,4], and **Hiroki Yokota**[1,2,*]

[1]Department of Biomedical Engineering, Indiana University – Purdue University Indianapolis, IN 46032, USA

[2]Department of Anatomy & Cell Biology, Indiana University – Purdue University Indianapolis, IN 46032, USA

[3]Graduate School of Natural Science and Technology, Kanazawa University, Ishikawa, Japan

[4]Department of Orthopaedic Surgery, Indiana University – Purdue University Indianapolis, IN 46032, USA

Abstract

Knee loading is a relatively new loading modality, where dynamic loads are laterally applied to the knee to induce bone formation in the tibia and the femur. The specific aim of the current study was to evaluate the effects of loading frequencies (in Hz) on bone formation at the site away from the loading site on the knee. The left knee of C57/BL/6 mice was loaded with 0.5-N force at 5, 10, or 15 Hz for 3 min/day for 3 consecutive days, and bone histomorphometry was conducted at the site 75% away from the loading site along the length of tibiae and femora. The results revealed frequency-dependent induction of bone formation, in which the dependence was different in the tibia and the femur. Compared to the sham-loading control, for instance, the cross-sectional cortical area was elevated maximally at 5 Hz in the tibia, whereas the most significant increase was observed at 15 Hz in the femur. Furthermore, mineralizing surface, mineral apposition rate, and bone formation rate were the highest at 5 Hz in the tibia (2.0-, 1.4-, and 2.7-fold, respectively) and 15 Hz in the femur (1.5-, 1.2-, and 1.8-fold, respectively). We observed that the tibia had a lower bone mineral density with more porous microstructures than the femur. Those differences may contribute to the observed differential dependence on loading frequencies.

Keywords

mechanical loading; knee joint; loading frequency; bone formation; femur; tibia

Introduction

Physical exercise has been shown to enhance mechanical strength of bone [1,2], and activities such as swimming [3], climbing [4,5], jumping [6], and whole-body vibration [7] are reported to increase bone mass. These activities are, however, mostly limited to healthy individuals [8] and their efficacy depends on an individual's weight, muscle strength, and fitness level. In order to understand the mechanism of load-driven bone formation and develop safe and

*Corresponding Author: Hiroki Yokota, PhD Indiana University – Purdue University Indianapolis (IUPUI) Fesler Hall 115 1120 South Drive Indianapolis, IN 46202 Phone: (317) 274-2448 Fax: (317) 278-9568 hyokota@iupui.edu.

The authors have no conflict of interest.

effective load-based therapies, various loading modalities have been investigated [9–13]. One of such modalities is joint loading, which has been recently shown as a unique means to stimulate trabecular and cortical bone formation [14–16]. Knee loading is one form of joint loading that applies lateral loads to synovial joints. The aim of the current study is to evaluate efficacy of knee loading at a site distant from the loading site on the knee and examine any dependence of its anabolic responses on loading frequencies in Hz.

Unlike most loading modalities such as four-point bending modality [9,10] and axial loading [11–13], joint loading does not depend on load-induced strain at a site of bone formation. Instead, loads are applied laterally to the epiphysis of the synovial joint for induction of bone formation in the diaphysis of long bone. Although its potential anabolic effects have been shown with elbow loading and knee loading, many questions on efficacy as well as loading conditions are unanswered. Here, we addressed a pair of questions: Is knee loading able to induce bone formation in the diaphysis distant from the knee in the tibia as well as in the femur? And if so, is load-driven induction affected by loading frequencies? Although the described loading modality does not provide habitual loads to the knee, its anabolic responses may contribute to strengthening bone and preventing bone loss to individuals who have limited capabilities of conducting routine exercises such as walking and jogging.

To answer the above questions, we conducted a series of loading experiments using mice as a model system. In evaluation of bone formation in the diaphysis away from the knee, we focused on the site 75% distant from the knee in the tibia and the femur along a length of those long bones. Dependence on loading frequencies has been pointed out in previous studies [12,13], but to our knowledge no comparative analysis for the tibia and the femur has been conducted. In addition, although loading frequencies above 10 Hz may occur during daily activities [17], there are few studies that have examined anabolic effects above 10 Hz. Thus, in this report we chose three loading frequencies at 5, 10, and 15 Hz. Many factors can be involved in dictating frequency responses of the tibia and the femur. In this paper we evaluated potential correlation of porosity and bone mineral density in the tibia and the femur to their frequency responses.

Materials and methods

Experimental animals

Fifty-four female C57/BL/6 mice, ~ 14 weeks of age (a body weight, ~ 20 g) were used (Harlan Sprague-Dawley, Inc., Indianapolis, IN). Four to five animals were housed per cage and fed with standard laboratory chow and water *ad libitum*. The animals were allowed to acclimate for 2 weeks before experimentation. All procedures were in accordance with the Institutional Animal Care and Use Committee guidelines.

Mechanical loading

The mouse was placed in an anesthetic induction-chamber to induce sedation and mask-anesthetized using 2% isoflurane. The custom-made piezoelectric mechanical loader was employed to apply lateral loads for 3 min/day for 3 consecutive days to the left knee in the lateral-medial direction (Fig. 1). The mice were randomly divided into three groups for three loading frequencies (5, 10, or 15 Hz, N = 8), and the loads with a peak-to-peak force of 0.5 N were applied. The right hindlimb was used as sham-loading control. After loading, the mouse was allowed normal cage activity.

Calcein labeling and sample harvest

Mice were given an intraperitoneal injection of calcein (Sigma, St. Louis, MO), a fluorochrome dye, at 30 μg/g body mass on days 2 and 6 after the last loading (Fig. 2). Animals were sacrificed 2 weeks after the last loading, and the left and right femora and tibiae were harvested for μCT

and histomorphometic analyses. The isolated bones were cleaned of soft tissues, and the distal and proximal ends were cleaved to allow infiltration of the fixatives with 10% neutral buffered formalin. After 48 h in the fixatives bones were transferred to 70% alcohol for storage.

μCT imaging

Micro-CT was performed using a desktop μCT-20 (Scanco Medical AG, Auenring, Switzerland) (see Fig. 5). The harvested tibiae and femora were placed in a plastic tube filled with 70% ethanol and centered in the gantry of the machine. A series of cross-sectional images were captured in a 3-mm segment at 30-μm resolution. Bone porosity of the tibial and femoral cortical bone was analyzed [18].

Bone histomorphometry

Specimens were dehydrated in a series of graded alcohols and embedded in methyl methacrylate (Aldrich Chemical Co., Milwaukee, WI). The transverse sections (~ 80 μm in thickness) were removed from the tibial shaft, ~12 mm (75%) distant from the proximal end of the tibia, and the femoral shaft, ~12 mm (75%) distant from the distal end of the femur using a diamond-embedded wire saw (Delaware Diamond Knives, Wilmington, DE). After polishing the surface they were mounted on standard microscope slides.

We measured total perimeter (B.Pm), endocortical perimeter, single-labeled perimeter (sL.Pm), double-labeled perimeter (dL.Pm), and double-labeled area (dL.Ar). From these measurements, we derived mineralizing surface (MS/BS = [1/2sL.Pm + dL.Pm]/B.Pm in %), mineral apposition rate (MAR = dL.Ar/dL.Pm/4 in μm/day), and bone formation rate (BFR/BS = MAR × MS/BS × 365 in $\mu m^3/\mu m^2$ per year). To evaluate the effects of loading frequencies, the relative parameters such as rMS/BS, rMAR, and rBFR/BS were derived as differences between the values from the loaded tibiae/femora and the non-loaded control tibiae/femora. The relative alteration was calculated as differences between the loaded (L) and control (C) samples such as ([L − C] / C × 100 in %).

To examine load-driven alteration in bone size, the total bone cross-sectional area (mm^2), bone medullary area (mm^2), and cortical thickness (mm) were measured. The cross-sectional cortical area was determined by subtracting the bone medullary area from the total bone cross-sectional area. The cortical thickness was defined as the mean distance between the endosteal surface and the periosteal surface on three sides (medial, lateral and posterior) for the tibia, or the anterior and posterior sides for the femur. The measurements were taken at the middle of each side, and the mean value was calculated from 2 independent measurements. We also determined BV/TV (bone area/total area in %) for cortical bone, and relative cortical thickness (cortical bone thickness/cross-sectional area).

Bone porosity, bone mineral density (BMD), and bone mineral content (BMC)

Intracortical porosity was determined from the tibial and the femoral transverse sections of the non-loaded limbs (N = 24). Using a Nikon Optiphot microscope and a Bioquant digitizing system, we measured cross-sectional cortical area (mm^2), total porous area (mm^2), and the number of pores with areas larger than 11 μm^2. From these measurements, we derived intracortical porosity (ratio of porous area to total bone area in %) and pore density (number/mm^2). Six age-match animals were used to determine the BMD and BMC of the entire tibiae and femurs (N = 12, including both left and right) with a PIXImus densitometer (software version 1.4×, GE Medical System Lunar, Madison, WI, USA) [19].

Statistical analysis

The data were expressed as mean ± SEM. Statistical significance among groups was examined using one-way ANOVA, and a post-hoc test was conducted using Fisher's protected least significant difference (PLSD) for the pair wise comparisons. A paired *t*-test was employed to evaluate statistical significance between the loaded and control samples. All comparisons were two-tailed and statistical significance was assumed for $p < 0.05$.

Results

The animals tolerated the procedures for the loading experiments, and any abnormal behavior including diminished food intake and weight loss was not observed. No bruising or other damage was detected at the loading site.

Load-driven alteration in cortical area and cortical thickness in the tibia

A frequency-dependent increase in cortical area and cortical thickness was observed (Fig. 3). The cross-sectional cortical area was increased from 0.56 ± 0.02 mm^2 (control) to 0.63 ± 0.01 mm^2 (loading) at 5 Hz ($p < 0.05$), and from 0.55 ± 0.02 mm^2 (control) to 0.61 ± 0.02 mm^2 (loading) at 10 Hz ($p < 0.05$). No significant alteration was observed at 15 Hz ($p = 0.107$). Similarly, the cortical thickness was elevated from 0.223 ± 0.004 mm (control) to 0.252 ± 0.006 mm (loading) at 5 Hz ($p < 0.01$) and from 0.218 ± 0.004 mm (control) to 0.236 ± 0.005 mm (loading) at 10 Hz ($p < 0.05$). No significant changes were observed at 15 Hz ($p = 0.177$). In the data combined for the three loading groups the cortical BV/TV increased from 0.667 ± 0.006 (control) to 0.694 ± 0.006 (loading) ($p < 0.01$) and so did the relative cortical thickness from 0.0265 ± 0.0004 (control) to 0.0277 ± 0.0003 (loading) ($p < 0.05$) (Fig. 3).

Load-driven alteration in cortical area and cortical thickness in the femur

In the femur a frequency response was different from the tibia (Fig. 3). The cortical area was enlarged from 0.75 ± 0.03 mm^2 (control) to 0.84 ± 0.01 mm^2 (loading) with a loading frequency at 15 Hz ($p < 0.01$), but unlike the tibia no significant alteration was observed at 5 Hz ($p = 0.619$) or 10 Hz ($p = 0.189$). The thickness was elevated from 0.201 ± 0.005 mm (control) to 0.223 ± 0.004 mm (loading) at 15 Hz ($p < 0.01$) and from 0.205 ± 0.004 mm (control) to 0.220 ± 0.004 mm (loading) at 10 Hz ($p < 0.05$). No significant changes were observed at 5 Hz ($p = 0.447$). In summary, the cortical BV/TV was increased from 0.461 ± 0.009 (control) to 0.488 ± 0.005 (loading) ($p < 0.05$) in the combined data for the three loading groups. The relative cortical thickness increased from 0.0121 ± 0.0002 (control) to 0.0129 ± 0.0002 (loading) ($p < 0.01$) (Fig. 3). The cross-sectional area of the tibia and the femur was increased with knee loading in all six loading bouts in the present study. However, statistically significance elevation was observed only in the tibia in response to loads applied at 5 Hz (from 0.83 ± 0.02 mm^2 to 0.90 ± 0.01 mm^2 with $p < 0.05$).

Bone morphometric parameters in the tibia

Bone formation in the periosteal surface was stimulated by knee loading at 5 Hz and 10 Hz (Table 1). Compared to the sham-loading control, loading at 5 Hz resulted in a significant increase in three morphometric parameters (2.0 × for MS/BS with $p < 0.01$, 1.4 × for MAR with $p < 0.001$, and 2.7 × for BFR/BS with $p < 0.01$). Similarly, the loading at 10 Hz elevated these parameters (1.7 × for MS/BS with $p < 0.05$, 1.3 × for MAR with $p < 0.01$, and 2.1 × for BFR/BS with $p < 0.05$). Likewise, bone formation on the endosteal surface was stimulated by knee loading but only at 5 Hz. Compared to the sham-loading control, three morphometric parameters were elevated (1.3 × for MS/BS with $p < 0.05$, 1.2 × for MAR with $p < 0.01$, and 1.5 × for BFR/BS with $p < 0.01$).

Bone morphometric parameters in the femur

Bone formation on the periosteal surface was significantly stimulated by knee loading at 10 and 15 Hz, but no statistical significance was observed on the endosteal surface (Table 2). Compared to the sham-loading control, the loading at 10 Hz elevated two of these parameters on the periosteal surface (1.2 × for MAR with $p < 0.05$, and 1.7 × for BFR/BS with $p < 0.05$). The loading at 15 Hz was the most effective and resulted in a significant increase in three morphometric parameters (1.5 × for MS/BS with $p < 0.05$, 1.2 × for MAR with $p < 0.05$, and 1.8 × for BFR/BS with $p < 0.05$). No statistical difference was observed with the loading at 5 Hz.

Dependence of anabolic responses on loading frequencies

Dependence on the loading frequencies was prominent in the relative parameters defined on the periosteal surface in the tibia (Fig. 4). Compared to loading at 15 Hz, loading at 5 Hz resulted in a significant increase in three morphometric parameters ($p < 0.01$ for rMS/BS, $p < 0.001$ for rMAR and rBFR/BS). Furthermore, compared to loading at 15 Hz, loading at 10 Hz resulted in an increase in these parameters ($p < 0.05$ for rMAR and rBFR/BS). Unlike the periosteal surface in the tibia, no significant loading effects were observed in the femur regarding those morphometric parameters ($p = 0.11 – 0.19$; data not shown).

In order to further examine the effects of knee loading on the periosteal surfaces in the tibia, rMS/BS, rMAR, and rBFR/BS were determined and normalized by the values of the control group (% of control). Based on the normalized change on the periosteal surface, loading at 5 Hz elevated rMAR ($p < 0.001$) and rBFR/BS ($p < 0.01$) more than loading at 15 Hz did. Furthermore, loading at 10 Hz resulted in a significant increase in rMAR and rBFR/BS (both $p < 0.05$) compared to loading at 15 Hz. Unlike the periosteal surface in the tibia no significant loading effects were observed in the femur for the morphometric parameters ($p = 0.20 – 0.29$; data not shown). Among the three frequencies employed in the study, bone formation in the tibia was most enhanced at the lowest frequency (5 Hz) while in the femur it was most effective at the highest frequency (15 Hz).

Bone porosity, BMD, and BMC

In order to evaluate any link of the observed frequency dependence to bone microstructure, we evaluated bone porosity as well as BMD and BMC. First, bone porosity in the cortical bone was significantly different between the tibia and femur (Fig. 5). The measurement of intracortical porosity revealed that the tibia (1.79 ± 0.10 %) was more porous than the femur (1.18 ± 0.04 %) ($p < 0.001$). Similarly, the porosity density (number/mm^2) was higher in the tibia (831 ± 42) than the femur (666 ± 20) ($p < 0.01$). Those observations were confirmed by μCT images, where the tibia presented the greater number of pores and more porous areas than the femur. Second, in age-match mice the value of BMD in the tibia (32.3 ± 0.7 mg/cm^2) was significantly lower than that in the femur (34.8 ± 0.5 mg/cm^2) ($p < 0.01$). In the BMC measurement, although the value in the tibia (8.1 ± 0.4 mg) was lower than the femur (8.9 ± 0.5 mg), no statistical significance was detected ($p > 0.05$).

Discussion

The present study reveals that knee loading induces formation of cortical bone on the periosteal and endosteal surfaces at a location considerably remote from the loading site. As a mechanism of induction of bone formation, we postulate that low-magnitude loads applied to the epiphysis alter pressure in the intramedullary cavity and this in turn influences intracortical fluid flow (Fig. 6) [20–24]. To examine possible induction of molecular transport with knee loading, we previously examined load-driven molecular transport using a fluorescence recovery after photo-bleaching technique [25]. In the experiment a lacuna in the diaphysis was photobleached,

and a time constant for recovering fluorescence signals was determined with and without knee loading. The results revealed that knee loading shortened the time constant. Furthermore, oscillatory alteration of intramedullary pressure in the femur was observed in response to sinusoidal loading with knee loading [26]. Taken together, knee loading appears to affect motion of interstitial fluid as well as medullary fluid.

The loading effects were dependent on loading-frequencies and the dependence was different in the tibia and the femur. In the tibia 5 and 10 Hz was more effective than 15 Hz, while in the femur induction was most significant at 15 Hz. Other studies indicate that the effective frequency differs depending on the loading modalities [17,27,28]. In whole-body vibration higher frequencies (> 30 Hz) have been suggested to be more effective [29,30]. Similarly, with ulna axial loading using rats bone formation was increasingly elevated with an increase in loading frequencies from 1 Hz to 10 Hz [28]. In contrast, with ulna axial loading using mice the frequencies at 5 and 10 Hz were reported to be more effective than 20 or 30 Hz [12].

A potential cause of differential frequency responses in the current study includes differences in transmission of force in the knee, size and shape of tibiae and femora, blood pressure and pressure in the lacunocanalicular network, viscoelastic characters, cellular and molecular environments, and microstructures such as porosity. Since the study by Qin *et al.* using turkey ulnae has showed that the rate of bone formation is correlated to a distribution of pores in a cross-section of turkey ulnae [31,32], we examined porosity of cortical bone of the tibia and the femur. Histological and μCT analyses revealed that cortical bone in the femur has a higher BMD with a fewer number of pores than the tibia. According to a poroelasticity theory, the observed difference in the pore volume fraction alters permeability of solutes in the lacunocanalicular network, compressibility of the poroelastic medium, and bulk modulus of the undrained poroelastic bone [33,34]. The difference should thereby affect nutrient transport, bone mineralization, and mechanotransduction. We observed that the tibia with a high pore fraction was responsive to a lower loading frequency than the femur. Further investigation is necessary to evaluate the linkage between porosity and frequency dependence in the tibia and the femur.

Porosity is directly linked to the size of osteocyte population, which influences activities in bone remodeling. Recent studies have suggested that the relationship between osteocyte density and bone formation rate varies depending on skeletal site and developmental history. In human cancellous bone the inverse relationship between osteocyte density and bone formation rate was reported [35], while in rat woven bone osteocytes were viewed as a local initiator of bone remodeling and remodeling at an accelerated rate was observed at high lacunar density [36]. Between the tibia and the femur in the present study the tibia exhibited higher bone formation rate at 5 and 10 Hz, and the femur at 15 Hz. Our results suggest that any relationship between osteocyte density and bone formation rate is apparently dependent on a loading condition

The present study presented differential sensitivity of the periosteal and endosteal surfaces in response to knee loading. We observed increased bone formation in the periosteum and the endosteum, but in contrast to the marked enhancement of bone formation on the periosteal surface, the endosteal surface exhibited no statistically significant increase except for the bout in the tibia at 5 Hz. Interestingly, the observations herein are consistent with some of the previous studies using other loading modalities such as axial loading [37,38], bending [39], climbing [5], running [40], and jumping [6]. The results may suggest a differential role of load-driven alterations in intramedullary pressure between the periosteal and endosteal surfaces. Alternatively, differences in anatomical and physiological microenvironments exist, and differential anabolic responses could result from variations in cellular and molecular

compositions as well as in heterogeneous propagation of load-driven pressure gradients and interstitial fluid flow.

In summary, the current study demonstrates that knee loading is an effective means to induce bone formation in the proximal diaphysis in the femur and the distal diaphysis in the tibia. Knee loading is a recently developed loading modality that could with further research provide potential for slowing bone loss in the femur and the tibia. Understanding the mechanism of bone formation with knee loading would contribute to future treatments and therapies for the promotion of bone quality.

Acknowledgments

The authors appreciate G.M. Malacinski for critical reading of the manuscript. This study was in part supported by NIH R03AG024596 and NIH R01AR52144.

References

1. Holy X, Zerath E. Bone mass increases in less than 4 wk of voluntary exercising in growing rats. Med Sci Sports Exerc 2000;32:1562–1569. [PubMed: 10994905]
2. Turner CH, Robling AG. Mechanisms by which exercise improves bone strength. J Bone Miner Metab 2005;23:S16–22.
3. Hart KJ, Shaw JM, Vajda E, Hegsted M, Miller SC. Swim-trained rats have greater bone mass, density, strength, and dynamics. J Appl Physiol 2001;91:1663–1668. [PubMed: 11568148]
4. Notomi T, Okimoto N, Okazaki Y, Tanaka Y, Nakamura T, Suzuki M. Effects of tower climbing exercise on bone mass, strength, and turnover in growing rats. J Bone Miner Res 2001;16:166–171. [PubMed: 11149481]
5. Mori T, Okimoto N, Sakai A, Okazaki Y, Nakura N, Notomi T, Nakamura T. Climbing exercise increases bone mass and trabecular bone turnover through transient regulation of marrow osteogenic and osteoclastogenic potentials in mice. J Bone Miner Res 2003;18:2002–2009. [PubMed: 14606513]
6. Kodama Y, Umemura Y, Nagasawa S, Beamer WG, Donahue LR, Rosen CR, Baylink DJ, Farley JR. Exercise and mechanical loading increase periosteal bone formation and whole bone strength in C57BL/6J mice but not in C3H/Hej mice. Calcif Tissue Int 2000;66:298–306. [PubMed: 10742449]
7. Flieger J, Karachalios T, Khaldi L, Raptou P, Lyritis G. Mechanical stimulation in the form of vibration prevents postmenopausal bone loss in ovariectomized rats. Calcif Tissue Int 1998;63:510–514. [PubMed: 9817946]
8. Chestnut CH. Bone mass and exercise. Amer J Med 1993;95:34S–36S. [PubMed: 8256792]
9. Pedersen EA, Akhter MP, Cullen DM, Kimmel DB, Recker RR. Bone response to in vivo mechanical loading in C3H/HeJ mice. Calcif Tissue Int 1999;65:41–46. [PubMed: 10369732]
10. Kameyama Y, Hagino H, Okano T, Enokida M, Fukata S, Teshima R. Bone response to mechanical loading in adult rats with collagen-induced arthritis. Bone 2004;35:948–956. [PubMed: 15454102]
11. Li J, Burr DB, Turner CH. Suppression of prostaglandin synthesis with NS-398 has different effects on endocortical and periosteal bone formation induced by mechanical loading. Calcif Tissue Int 2002;70:320–329. [PubMed: 12004337]
12. Warden SJ, Turner CH. Mechanotransduction in cortical bone is most efficient at loading frequencies of 5–10 Hz. Bone 2004;34:261–270. [PubMed: 14962804]
13. Hsieh YF, Robling AG, Ambrosius WT, Burr DB, Turner CH. Mechanical loading of diaphyseal bone in vivo: the strain threshold for an osteogenic response varies with location. J Bone Miner Res 2001;16:2291–2297. [PubMed: 11760844]
14. Tanaka SM, Sun HB, Yokota H. Bone formation induced by a novel form of mechanical loading on joint tissue. Biol Sci Space 2004;18:41–44. [PubMed: 15308820]
15. Yokota H, Tanaka SM. Osteogenic potential with joint loading modality. J Bone Miner Metab 2005;23:302–308. [PubMed: 15981026]
16. Zhang P, Tanaka SM, Jiang H, Su M, Yokota H. Diaphyseal bone formation in murine tibiae in response to knee loading. J Appl Physiol 2006;100:1452–1459. [PubMed: 16410382]

17. Turner CH, Yoshikawa T, Forwood MR, Sun TC, Burr DB. High frequency components of bone strain in dogs measured during various activities. J Biomech 1995;28:39–44. [PubMed: 7852440]
18. Jove G, Michael R, Lisa P. Effect of Bone Porosity on the Mechanical Integrity of the Bone-Cement Interface. J Bone Joint Surg Am 2003;85:1901–1908. [PubMed: 14563796]
19. Alam I, Warden SJ, Robling AG, Turner CH. Mechanoransduction in bone does not require a functional cyclooxygenase-2 (COX-2) gene. J Bone Miner Res 2005;20:438–446. [PubMed: 15746988]
20. Burr DB, Robling AG, Turner CH. Effects of biomechanical stress on bones in animals. Bone 2002;30:781–786. [PubMed: 11996920]
21. Knothe Tate ML, Knothe U. An ex vivo model to study transport processes and fluid flow in loaded bone. J Biomech 2000;33:247–254. [PubMed: 10653041]
22. Tami AE, Nasser P, Verborgt O, Schaffler MB, Knothe Tate ML. The role of interstitial fluid flow in the remodeling response to fatigue loading. J Bone Miner Res 2002;17:2030–2037. [PubMed: 12412811]
23. Montgomery RJ, Sutker BD, Bronk JT, Smith SR, Kelly PJ. Interstitial fluid flow in cortical bone. Microvasc Res 1988;35:295–307. [PubMed: 3393091]
24. Warden SJ. Breaking the rules for bone adaptation to mechanical loading. J Appl Physiol 2006;100:1441–1442. [PubMed: 16614362]
25. Su M, Jiang H, Zhang P, Liu Y, Wang E, Hsu A, Yokota H. Knee-loading modality drives molecular transport in mouse femur. Ann Biomed Eng 2006;34:1600–1606. [PubMed: 17029032]
26. Zhang P, Su M, Liu Y, Hsu A, Yokota H. Knee loading dynamically alters intramedullary pressure in mouse femora. Bone 2007;40:538–543. [PubMed: 17070127]
27. Rubin CT, McLeod KJ. Promotion of bony ingrowth by frequency-specific, low-amplitude mechanical strain. Clin Orthop Rel Res 1994;298:165–174.
28. Hsieh YF, Turner CH. Effects of loading frequency on mechanically induced bone formation. J Bone Miner Res 2001;16:918–924. [PubMed: 11341337]
29. Rubin C, Turner AS, Bain S, Mallinckrodt C, McLeod KA. Low mechanical signals strengthen long bones. Nature 2001;412:603–604. [PubMed: 11493908]
30. Rubin C, Recker R, Cullen D, Ryaby J, McCabe J, McLeod K. Prevention of postmenopausal bone loss by a low-magnitude, high-frequency mechanical stimuli: a clinical trial assessing compliance, efficacy, and safety. J Bone Miner Res 2004;19:343–351. [PubMed: 15040821]
31. Qin YX, Kaplan T, Saldanha A, Rubin CT. Fluid pressure gradients, arising from oscillations in intramedullary pressure, is correlated with the formation of bone and inhibition of intracortical porosity. J Biomech 2003;36:1427–1437. [PubMed: 14499292]
32. Qin YX, Lin W, Rubin C. The pathway of bone fluid flow as defined by in vivo intramedullary pressure and streaming potential measurements. Ann Biomed Eng 2002;30:693–702. [PubMed: 12108843]
33. Cowin SC. Bone poroelasticity. J Biomech 1999;32:217–238. [PubMed: 10093022]
34. Swan CC, Lakes RS, Brand RA, Stewart KJ. Micromechanically based poroelastic modeling of fluid flow in Haversian bone. J Biomech Eng 2003;125:25–37. [PubMed: 12661194]
35. Qiu S, Rao DS, Palnitkar S, Parfitt AM. Relationships between osteocyte density and bone formation rate in human cancellous bone. Bone 2002;31:709–711. [PubMed: 12531566]
36. Hernandez CJ, Majeska RJ, Schaffler MB. Osteocyte density in woven bone 2004;35:1095–1099.
37. Lee KC, Maxwell A, Lanyon LE. Validation of a technique for studying functional adaptation of the mouse ulna in response to mechanical loading. Bone 2002;31:407–412. [PubMed: 12231414]
38. De Souza RL, Matsuura M, Eckstein F, Rawlinson SC, Lanyon LE, Pitsillides AA. Non-invasive axial loading of mouse tibiae increases cortical bone formation and modifies trabecular organization: a new model to study cortical and cancellous compartments in a single loaded element. Bone 2005;37:810–818. [PubMed: 16198164]
39. LaMothe JM, Hamilton NH, Zernicke RF. Strain rate influences periosteal adaptation in mature bone. Med Eng Phys 2005;27:277–284. [PubMed: 15823468]

40. Wu J, Wang XX, Higuchi M, Yamada K, Ishimi Y. High bone mass gained by exercise in growing male mice is increased by subsequent reduced exercise. J Appl Physiol 2004;97:806–810. [PubMed: 15090485]

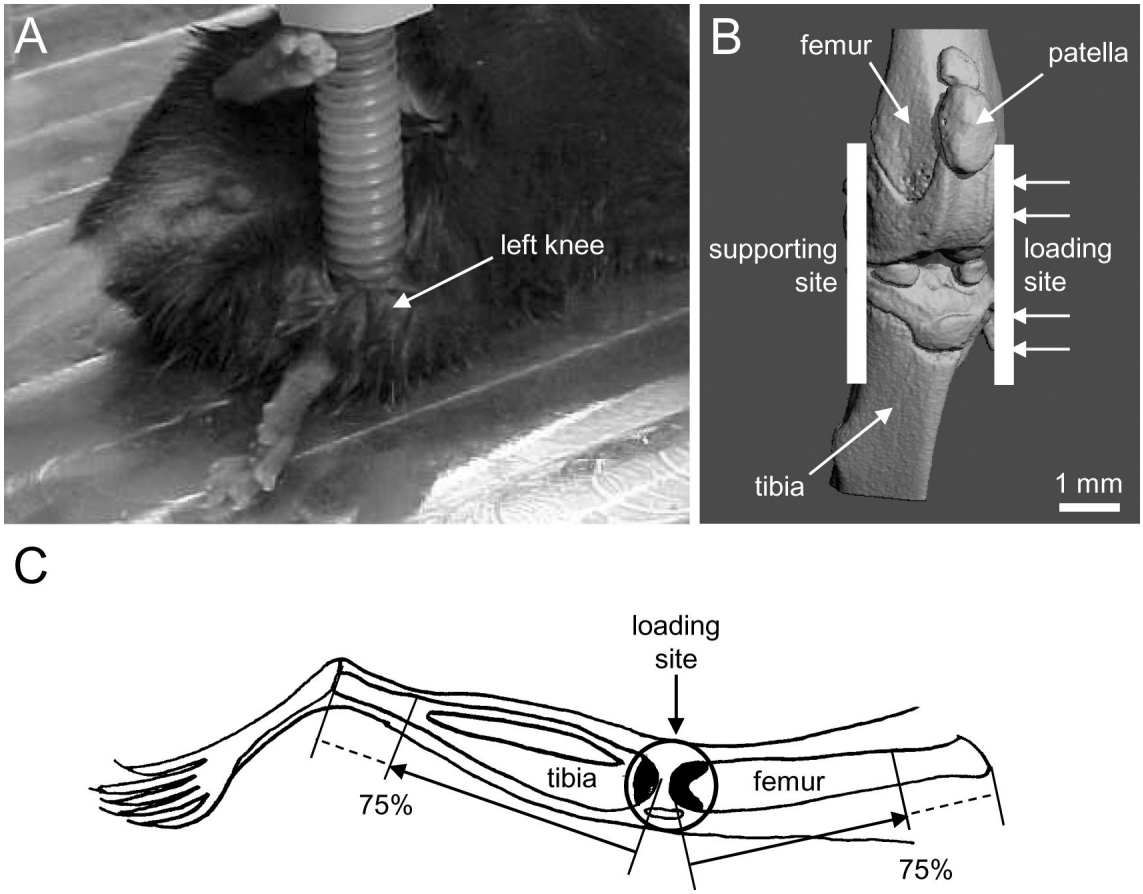

Fig. 1.

Setup of the mechanical loader used in this study. **A** Custom-made mechanical loader with a mouse mounted on the table. **B** Micro CT image illustrating the loading site to the tibia and the femur. Bar = 1 mm. **C** Hindlimb showing the tibial and femoral diaphysis (bone formation site; 75% along the length of the tibia and the femur) and the loading site in the epiphysis.

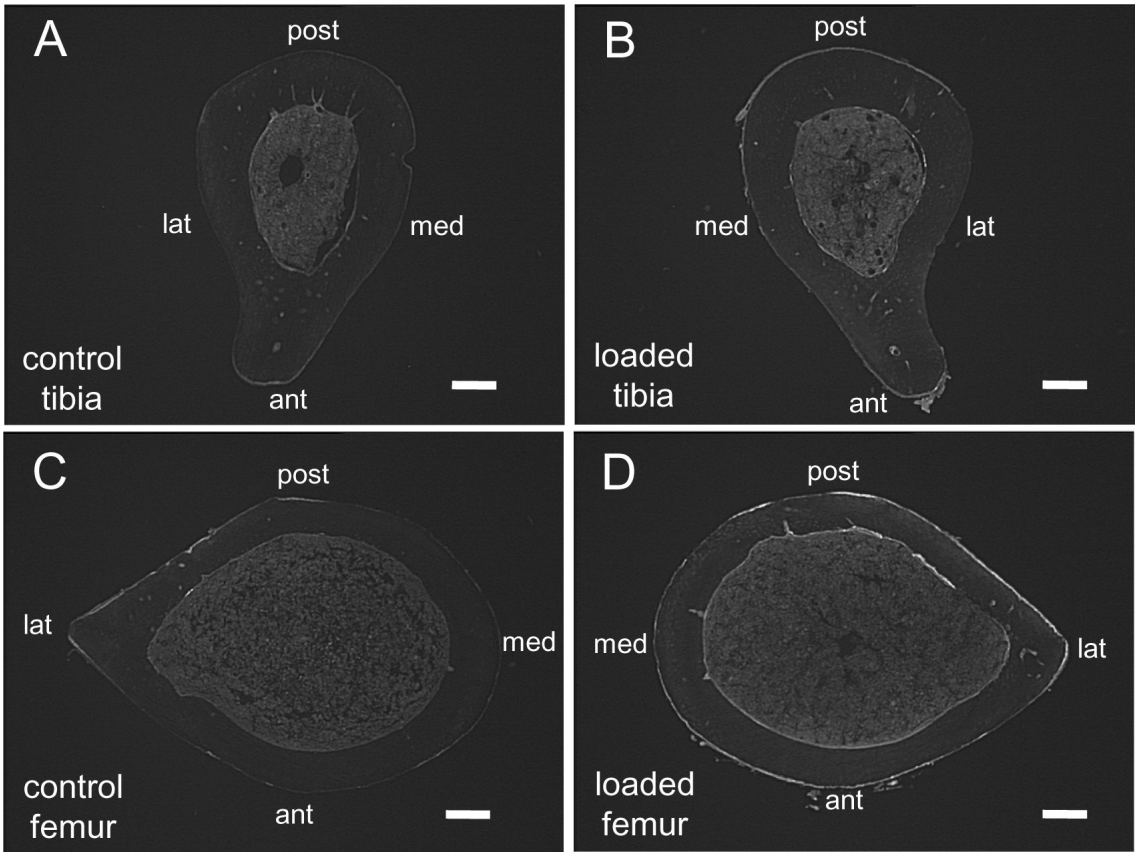

Fig. 2.

Tibial and femoral sections. The labels are medial (med), lateral (lat), anterior (ant), and posterior (post). White bar = 200 μm. **A** Control tibia. **B** Loaded tibia at 5 Hz. The section was obtained ~ 12 mm distant from the proximal end of the tibia. **C** Control femur. **D** Loaded femur at 15 Hz. The section was obtained from ~ 12 mm distant from the distal end of the femur.

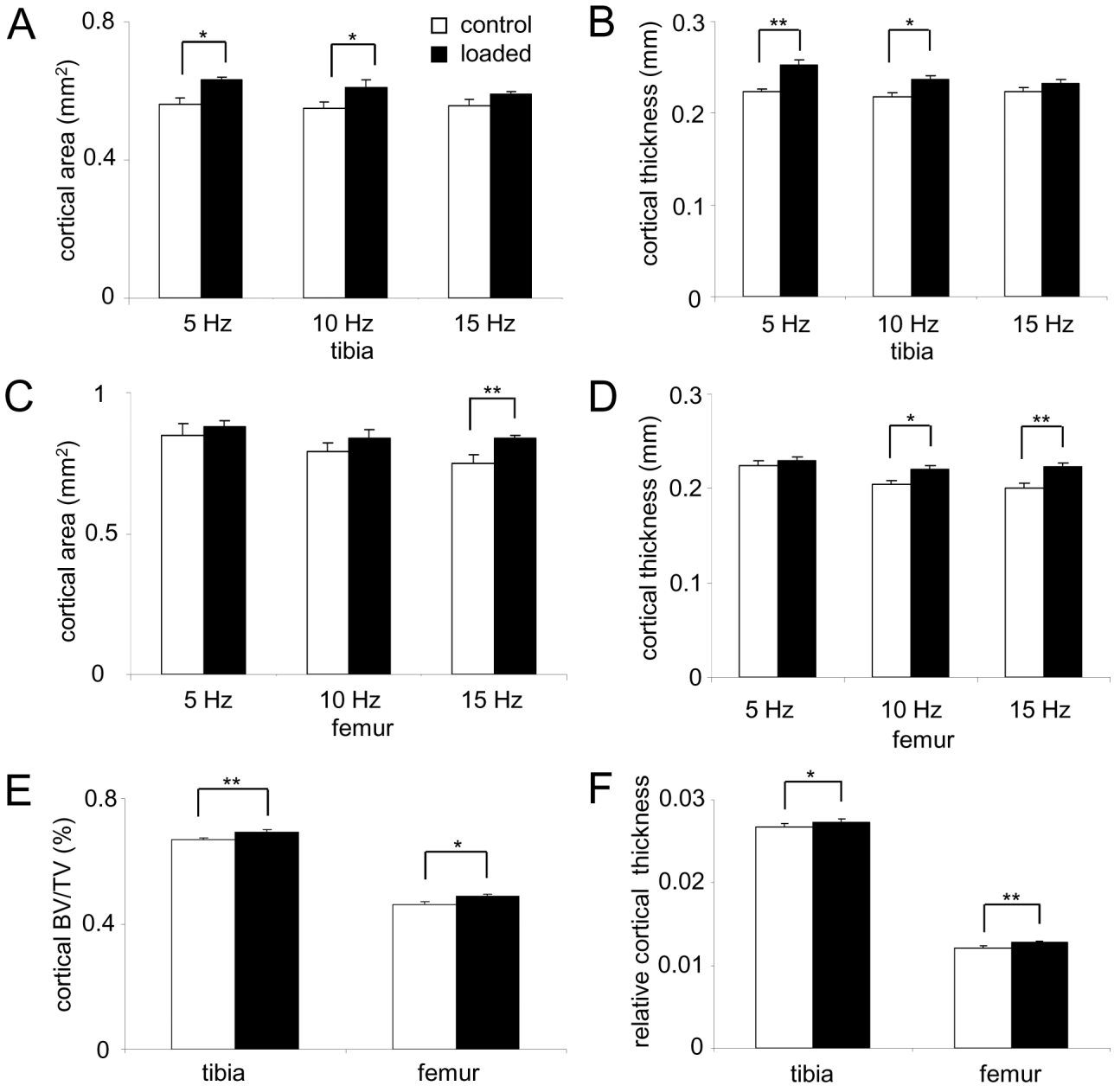

Fig. 3.

Alteration in the cross-sectional cortical area and cortical thickness with and without knee loading at 5, 10, and 15 Hz. The single and double asterisks indicate $p < 0.05$ and $p < 0.01$, respectively. **A** Cross-sectional cortical area (mm^2) in the tibia. **B** Cortical thickness (mm) in the tibia. **C** Cross-sectional cortical area (mm^2) in the femur. **D** Cortical thickness (mm) in the femur. **E** Cortical BV/TV (%) for the tibia and the femur. **F** Relative cortical thickness for the tibia and the femur.

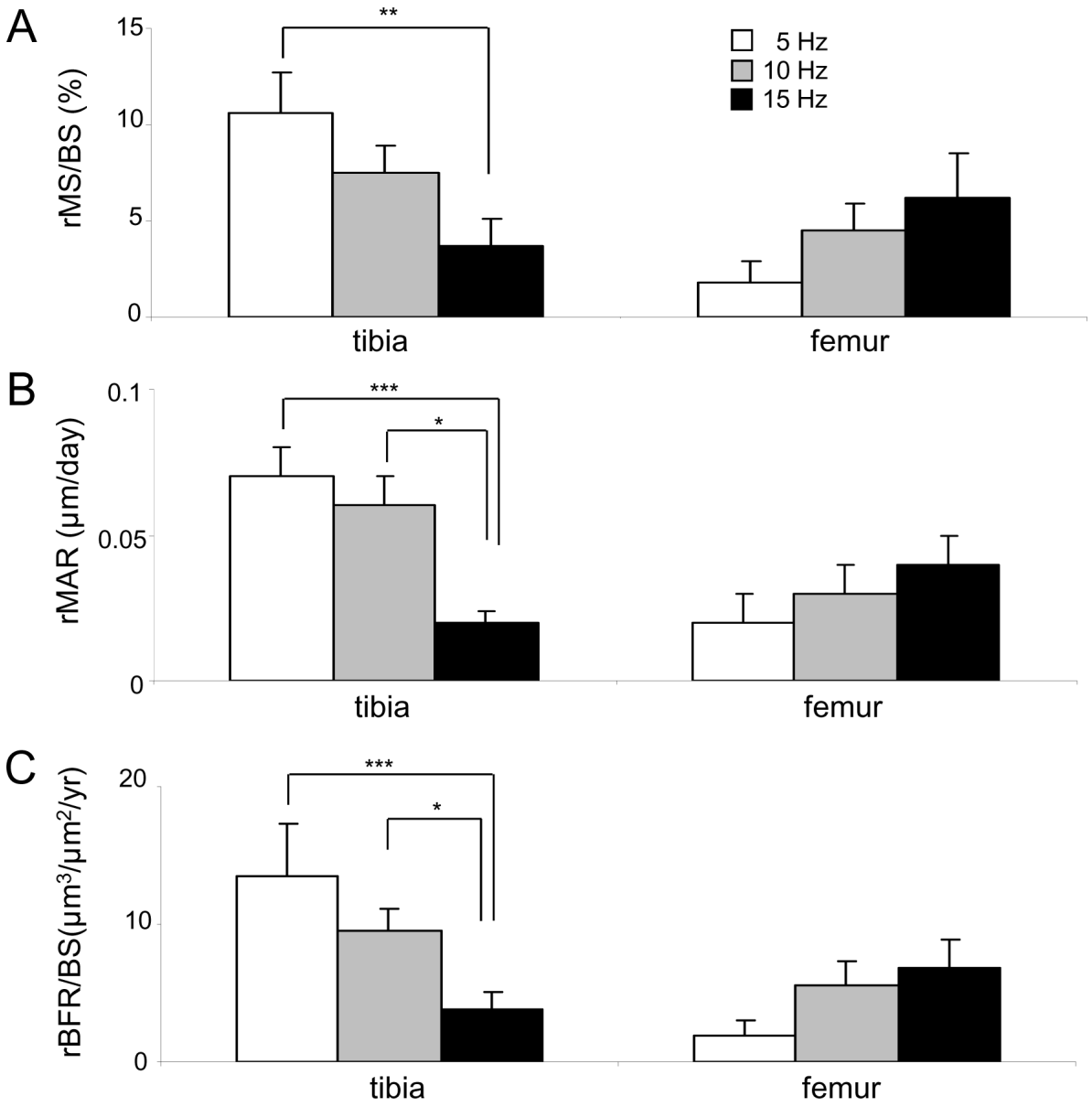

Fig. 4.

Alteration in the relative histo-morphometric parameters on the periosteal and endosteal surfaces with knee loading at 5, 10, and 15 Hz. The single, double, and triple asterisks indicate $p < 0.05$, $p < 0.01$ and $p < 0.001$, respectively. **A** Relative MS/BS (%). **B** Relative MAR (μm/day). **C** Relative BFR/BS ($\mu m^3/\mu m^2/yr$).

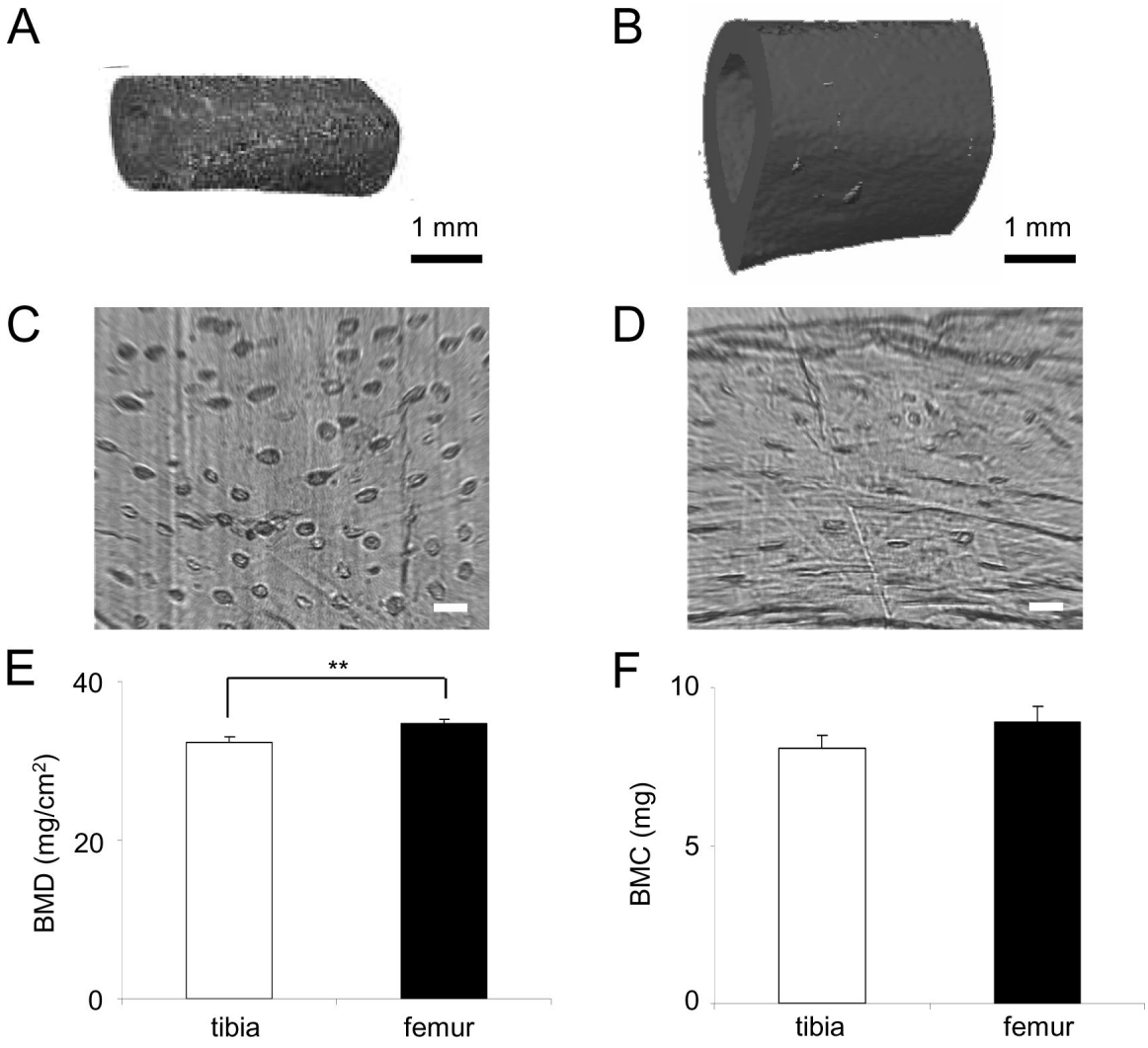

Fig. 5.

Bone porosity in the tibia and the femur. **A** 3D reconstruction of μCT image of the tibia. **B** 3D reconstruction of μCT image of the femur. **C** Tibial cross-section with pores. Bar = 20 μm. **D** Femoral cross-section with pores. Bar = 20 μm. **E** BMD for the tibia and the femur. **F** BMC for the tibia and the femur.

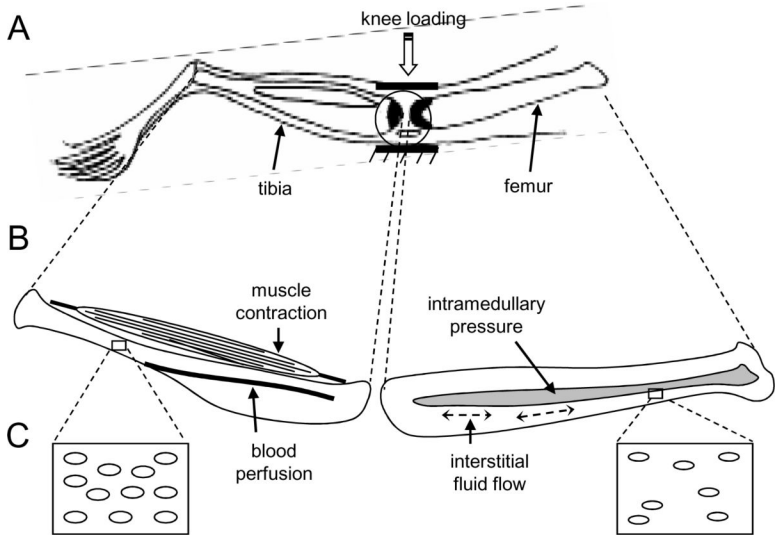

Fig. 6.

Potential contributors to the enhancement of bone formation in the femur with knee loading. This schematic illustration includes alteration in intramedullary pressure, muscle contraction, activation of blood perfusion, and load-driven interstitial fluid flow.

Table 1

Bone formation with the loading frequencies at 5 – 15 Hz in the tibia

		MS/BS (%)	*p* value	MAR (μm/day)	*p* value	BFR/BS ($\mu m^3/\mu m^2/yr$)	*p* value
5 Hz							
Periosteum	control	11.15±1.40		0.20±0.01		8.13±1.30	
	knee loading	21.79±2.51	<0.01	0.27±0.01	<0.001	21.64±2.78	<0.01
Endosteum	control	12.34±1.07		0.20±0.01		9.05±0.95	
	knee loading	16.23±1.13	<0.05	0.23±0.01	<0.01	13.92±1.18	<0.01
10 Hz							
Periosteum	control	11.34±2.65		0.21±0.01		8.80±2.16	
	knee loading	18.84±2.20	< 0.05	0.26±0.01	<0.01	18.32±2.56	< 0.05
Endosteum	control	11.81±2.80		0.20±0.01		8.40±1.89	
	knee loading	14.87±3.24	NS	0.23±0.01	NS	12.00±2.55	NS
15 Hz							
Periosteum	control	10.16±1.55		0.20±0.01		7.63±1.34	
	knee loading	13.91±2.31	NS	0.22±0.01	NS	11.46±2.12	NS
Endosteum	control	11.57±1.09		0.20±0.01		8.48±0.99	
	knee loading	14.12±1.52	NS	0.22±0.01	NS	11.32±1.52	NS

NS indicates $p > 0.05$.

Table 2

Bone formation with the loading frequencies at 5 – 15 Hz in the femur

		MS/BS (%)	*p* value	MAR (μm/day)	*p* value	BFR/BS ($\mu m^3/\mu m^2/yr$)	*p* value
5 Hz							
Periosteum	control	12.42±1.06		0.17±0.01		7.98±0.82	
	knee loading	14.20±0.75	NS	0.19±0.01	NS	9.91±0.74	NS
Endosteum	control	13.35±1.01		0.19±0.01		9.31±0.67	
	knee loading	14.88±1.47	NS	0.20±0.01	NS	11.13±1.22	NS
10 Hz							
Periosteum	control	13.11±1.00		0.18±0.01		8.57±0.86	
	knee loading	17.60±2.30	NS	0.21±0.01	< 0.05	14.15±2.45	< 0.05
Endosteum	control	11.77±2.56		0.19±0.01		8.07±1.86	
	knee loading	13.52±2.43	NS	0.20±0.01	NS	10.61±2.61	NS
15 Hz							
Periosteum	control	13.10±1.80		0.18±0.01		8.60±1.23	
	knee loading	19.32±1.85	< 0.05	0.22±0.01	< 0.05	15.50±2.03	< 0.05
Endosteum	control	13.42±1.15		0.18±0.01		8.86±0.74	
	knee loading	15.99±1.32	NS	0.20±0.01	NS	11.67±1.10	NS

NS indicates $p > 0.05$.